Research Article | Vol. 9, No. 7 / 1 July 2019 / Optical Materials Express 2797

Optical Materials EXPRESS

Low-loss planar optical waveguides based on plasma deposited silicon oxycarbide

LARS BAUDZUS* AND PETER M. KRUMMRICH

TU Dortmund, Chair for High Frequency Technology, Friedrich-Wöhler-Weg 4, 44227 Dortmund, Germany
*lars.baudzus@tu-dortmund.de

Abstract: Silicon oxycarbide deposited by plasma enhanced chemical vapor deposition is investigated regarding its application as a material for optical waveguides. The dependence of the infrared absorption, the refractive index, and the surface roughness on the precursor gas flow ratios is studied by Fourier transform infrared spectroscopy, ellipsometry, and atomic force microscopy, respectively. Results show that the refractive index can be tuned over a significant wider range compared to silicon oxynitride. Fabricated waveguides with a refractive index contrast of 0.05 show waveguide attenuation from about 0.3 dB/cm to 0.4 dB/cm for wavelengths between 1480 nm and 1570 nm. These low values were achieved without using a high temperature annealing process.

© 2019 Optical Society of America under the terms of the OSA Open Access Publishing Agreement

1. Introduction

Silicon based low-loss optical waveguide technologies enable a cost efficient wafer scale production of photonic integrated circuits for a wide range of applications. Besides multiplexers [1] and filter components [2] for optical communication systems, they find application as laser resonators [3], filters for spectroscopy [4] and imaging [5], and optical signal processors [6]. They can also be used for frequency comb [7] and supercontinuum generation [8] due to their nonlinear properties.

Chemical vapor deposition is the preferred process technology to realize low-loss waveguides with a high index contrast. Silicon nitride (SiN) [9] and silica waveguides [2,10,11] have been studied intensively. However, the use of typical precursor gases like SiH_4, SiH_2Cl_2 or NH_3 leads to hydrogenated films. The overtones of the vibrational modes of hydrogen bonds in these films can cause strong absorption in important wavelength bands like the optical C band. Especially the first overtone of the stretching N-H vibrational mode absorbing around 1510 nm is problematic [12]. Different methods have been proposed to circumvent this problem. On the one hand, hydrogen containing precursors can be replaced by halogenated or deuterated counterparts [13,14]. On the other hand, an annealing process at temperatures over 1100 °C can be used to drive out the hydrogen [12]. However, the latter approach is problematic, because the differences in the thermal expansion coefficients cause high mechanical stress which can induce birefringence and can lead to cracks [12]. The possible refractive index profiles are limited, since this issue gets more serious with higher refractive indices and film thicknesses.

Compared to hydrogenated SiN or silicon oxynitride (SiON) the hydrogen bonds in hydrogenated silicon oxycarbide (SiOC) are more favorable regarding the absorption in the optical C band [15]. The only absorption feature in the optical C band is caused by the second overtone of the stretching vibrational mode of the Si-H bond. Since the N-H bond has a first overtone close to the C Band, the impact of the Si-H bond is expected to be much lower. This opens the possibility to circumvent the high temperature annealing process. Another advantage of SiOC is the greater tuneability of the refractive index, since silicon carbide (SiC) has a significantly higher refractive index than SiN. At 630 nm the values are 2.55 for SiC and 2.0 for SiN. Besides these benefits, SiOC has been proposed as a convenient material for optical amplifiers when it is

#360501 https://doi.org/10.1364/OME.9.002797
Journal © 2019 Received 19 Feb 2019; revised 31 Mar 2019; accepted 1 Apr 2019; published 6 Jun 2019

doped with erbium ions. A photoluminescence up to 20 times higher compared to a SiO_2 host has been demonstrated [16].

In contrast to SiOC waveguides fabricated with magnetron sputtering exhibiting waveguide attenuations around 4 dB/cm [17] this study focuses on waveguides fabricated with a plasma-enhanced chemical vapor deposition (PECVD) process. Although, the idea to realize optical waveguides with PECVD SiOC is described in [15], to the best of our knowledge, we are the first who present results from an experimental investigation on the waveguide attenuation. There are several studies on PECVD SiOC deposited with organosilicon precursors especially for the application as as low-k dielectric [18]. However, while organosilicon precursors lead to porous films, small hydrocarbons like CH_4 as carbon source enable dense films suitable for low loss optical waveguides [15].

In section two of this article, the dependence of the infrared absorption, the refractive index, and the surface roughness on the precursor gas flow ratios is presented. The fabrication process and measured properties of SiOC waveguides are described and discussed in section three.

2. Optical properties and deposition parameters

An ideal material for optical waveguide application has few or no chemical bonds leading to absorption in the considered wavelength band. When these bonds cannot be prevented, their impact has to be minimized by properly chosen fabrication parameters. Especially the gas flow ratios of the PECVD process are crucial for the material composition. Therefore, their influence was investigated with attenuated total reflection (ATR) Fourier transform infrared spectroscopy (FTIR).

SiOC thin films with a thickness of 3 μm were deposited on silicon substrates in an Oxford Plasma System 100. The gases CH_4, CO_2, and SiH_4 diluted 5% in Ar were used. The considered gas flow ratios of SiH_4 and CH_4 are 2.5 sccm/100 sccm, 5 sccm/100 sccm, and 10 sccm/100 sccm. The refractive index was set to 1.67 at 633 nm for each sample by adjusting the CO_2 gas flow to ensure comparable reflective properties. The corresponding CO_2 gas flows were 160 sccm, 300 sccm, and 650 sccm, respectively. The rule that an increased CO_2 gas flow leads to a decreased refractive index and vice versa is valid for all SiH_4/CH_4 ratios, which enables the realization of the same refractive index for all three ratios. A power of 100 W was applied to the top electrode for all deposition processes. The substrate electrode has a diameter of 205 mm. The pressure of all processes was 1000 mTorr and the temperature 390 °C.

The results of the ATR FTIR measurements are depicted in Fig. 1. The absorptions by the stretching vibrational modes of the hydrogen bonds lie in the wavenumber range between 3800 cm^{-1} and 2000 cm^{-1}. The absorption bands around 3630 cm^{-1}, 2920 cm^{-1}, and 2166 cm^{-1} can be attributed to the Si-O-H, C-H, and Si-H bonds, respectively [19]. The obvious trend is that with an increasing SiH_4/CH_4 ratio the absorption by the Si-H bond increases while the absorption by the C-H bond decreases. The change of the gas flow ratio shows no significant effect on the absorption by the Si-O-H bond.

The wavenumber range between 1500-600 cm^{-1} contains two main absorption bands around 960 cm^{-1} and 740 cm^{-1} which can be attributed to the Si-O and Si-C stretching vibrational modes [19]. While the shape of the absorption spectra is similar for the gas flow ratios 2.5/100 and 5/100, the absorption spectrum for the ratio 10/100 shows a higher absorption by the Si-O bond. In general, an increased oxygen content results in a reduction of the refractive index. But since the SiOC films on all samples have the same refractive index, this is a sign for excess silicon in form of Si-Si bonds. The similarity of the other two spectra implies no excess silicon. Silicon atoms are foremost bond to carbon or oxygen.

The composition of PECVD SiOC can be finely tuned by the gas flow ratios over a wide range. When we do not consider silicon rich SiOC, the refractive index can be set to values between the

Optical Materials EXPRESS

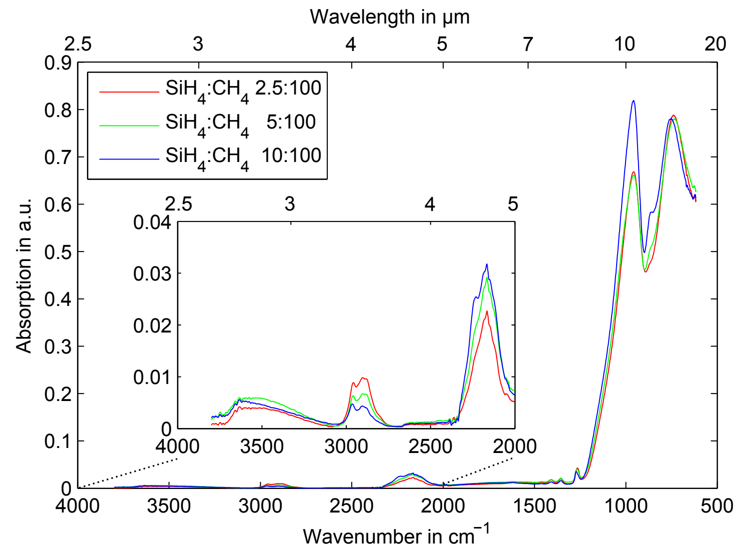

Fig. 1. ATR FTIR Spectrum of SiOC with an refractive index of 1.67 for different gas flow ratios of SiH_4 and CH_4.

refractive indices of SiO_2 and SiC. This feature enables application tailored waveguide designs which is especially important in hybrid technologies [20].

The refractive indices of SiOC thin films produced with different gas flows of CO_2 were measured by ellipsometry at 633 nm. Thin films with thicknesses between 70 and 100 nm were deposited on silicon substrates. For each deposition the SiH_4 and CH_4 gas flows were 5 sccm and 100 sccm, respectively. The power was 100 W, the pressure 1000 mTorr, and the temperature 390 °C.

The ellipsometer measurement results are shown in Fig. 2. The relationship between the CO_2 gas flow and the refractive index is nearly exponential. The values range from 1.5 to 2.33. The highest value corresponds to hydrogenated SiC and is lower than stoichiometric SiC which has a refractive index of 2.55. This is explained by excess carbon and the hydrogen content. Especially the absence of oxygen in the plasma can lead to an excess of carbon.

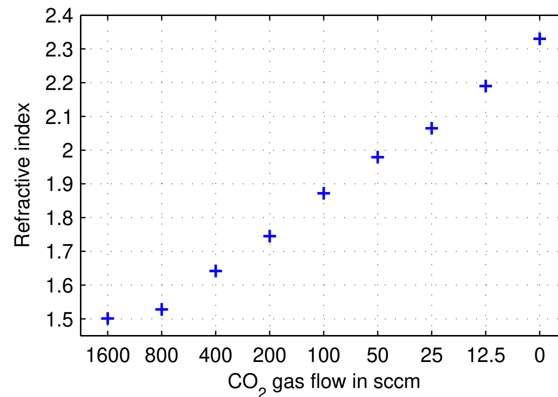

Fig. 2. Refractive index at 633 nm in dependence of the CO_2 gas flow with a SiH_4 gas flow of 5 sccm and a CH_4 gas flow of 100 sccm.

Optical Materials EXPRESS

Refractive indices higher than 2.33 can be achieved by increasing the SiH_4/CH_4 ratio. Though the transition to SiC with excess silicon is smooth. A reduction of the SiH_4/CH_4 leads to values below 1.5. When solely SiH_4 and CO_2 are used the refractive can be as low as 1.47.

Roughness at the interfaces between the waveguide core and cladding can be a major source of attenuation. While sidewall roughness mainly depends on the individual lithography and etching processes, surface roughness is caused by the deposition process. AFM was used to measure the surface profile and to determine the RMS roughness denoted as R_{RMS}.

Thin films with a thickness of 1 µm and five different refractive indices were deposited on silicon substrates. The pressure, power, and temperature were 1000 mTorr, 100 W, and 390 °C, respectively. The SiH_4 and CH_4 gas flows were 5 sccm and 100 sccm, respectively. These parameters were the same for all depositions. The values for the CO_2 gas flow were 1200 sccm, 280 sccm, 90 sccm, 25 sccm and, 0 sccm which lead to films with refractive indices at 630 nm of 1.52, 1.68, 1.87, 2.06, and 2.32.

The results of the AFM measurements are depicted in Fig. 3. The lowest roughness has the film with the refractive index 1.52 and the highest the one with 1.68. The roughness decreases with an increasing refractive index for values over 1.68. This leads to the insight that SiOC films with a more balanced composition of oxygen and carbon exhibit a higher roughness than films closer to SiO_2 and SiC. However, all measured roughness values are low enough to consider surface roughness as a minor source of attenuation [21]. The complete refractive index range can be considered for the realization of low-loss optical waveguides.

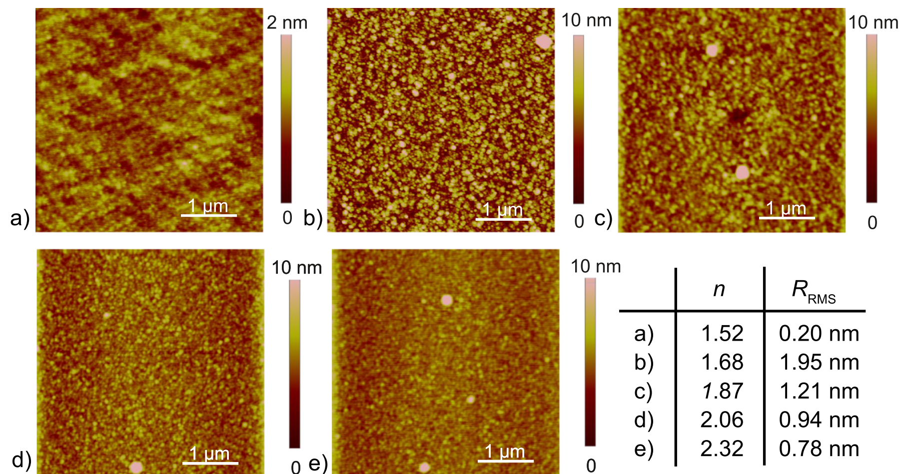

	n	R_{RMS}
a)	1.52	0.20 nm
b)	1.68	1.95 nm
c)	1.87	1.21 nm
d)	2.06	0.94 nm
e)	2.32	0.78 nm

Fig. 3. AFM measurement results for films with a thickness of 1 µm and different refractive indices.

3. Waveguide losses

The waveguide design is based on previous studies on PECVD SiON waveguides to allow a direct comparison [2,12]. The refractive index profile is depicted in Fig. 4. The refractive indices are given at 1550 nm. This waveguide design enables bending radii below 550 µm and fiber to chip coupling losses below 0.5 dB per facet [2].

The first step of the fabrication process is the deposition of 2 µm SiOC on a thermally oxidized 4" silicon wafer. The gas flows for SiH_4, CH_4, and CO_2 were 5 sccm, 100 sccm, and 1200 sccm, respectively. A pressure of 1200 mTorr, a power of 100 W, and a temperature of 390 °C were used. The waveguides were formed by broadband UV contact lithography and reactive ion etching with the gases CHF_3, O_2, and Ar. The top cladding was deposited by PECVD with the

Optical Materials EXPRESS

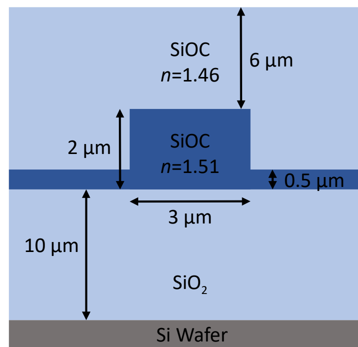

Fig. 4. Refractive index profile of the fabricated waveguides.

gas flows 5 sccm and 1500 sccm for SiH_4 and CO_2, respectively. The pressure was set to 1500 mTorr, the power to 100 W, and the temperature to 390 °C. Finally, the wafer was separated into chips and the facets were polished.

One of the insights of the ATR FTIR investigations presented in section two is that a low SiH_4/CH_4 ratio is preferable, because Si-H bonds absorbing in the optical C band are less pronounced in this case. However, the gas flow ratio 5 sccm/100 sccm was chosen over 2.5 sccm/100 sccm, because a minimum SiH_4 gas flow is necessary to achieve a uniform film thickness distribution on a 4" wafer. Increasing the CH_4 was not an option, because 100 sccm was the maximum flow of the available CH_4 mass flow controller. The pressure values used for the deposition of the waveguide core and cladding materials differ from the value used in section two, because they were optimized regarding the film thickness uniformity on a 4" wafer.

In addition to the photonic chip fabrication, the top cladding and the core material were each deposited on silicon substrates with a film thickness of 3 µm for ATR FTIR measurements. As seen in Fig. 5, SiOC deposited without CH_4 with a refractive index of 1.46 does not exhibit an absorption by C-H bonds, but has a more distinct absorption by Si-O-H bonds. The shape of the absorption bands caused by hydrogen bonds in the waveguide core material is comparable to the shapes seen in Fig. 1 where films with higher refractive indices were studied. As expected, the absorption by Si-O bonds increases with decreasing refractive index and the absorption by Si-C bonds decreases. The presence of Si-H bonds in the waveguide core and cladding materials indicates that both materials contribute to the waveguide attenuation.

Waveguides with four different lengths were fabricated to determine the waveguide attenuation and the coupling losses at each wavelength. The lengths were 2.5, 4.5, 5.9, and 7.1 cm. The waveguide chips were placed on a vacuum holder and Nufern UHNA4 fibers were positioned in front of the integrated waveguides by piezo actuators. No index matching gel was used between the fibers and the chip facets. A laser with a tuning range from 1480-1570 nm and an optical power meter were used to measure the losses. A photo of one of the chips is shown in Fig. 6. Meander structures were used to enable different waveguide lengths on one chip. The losses by the bendings with 500 µm radius can be neglected [2].

The waveguide attenuation was calculated from measured fiber to fiber transmission spectra of waveguides with four different lengths. Transmission spectra of waveguides with the lengths 2.5 cm and 7.1 cm are shown in Fig. 7 to illustrate the data basis for the calculation of the attenuation. A linear regression was applied to the data for each wavelength to determine the fiber to chip coupling losses from the offset parameter. The transmission spectra were subtracted by the average coupling loss and then divided by their corresponding length. For each wavelength the attenuation is determined by averaging and the standard error is calculated.

Optical Materials EXPRESS

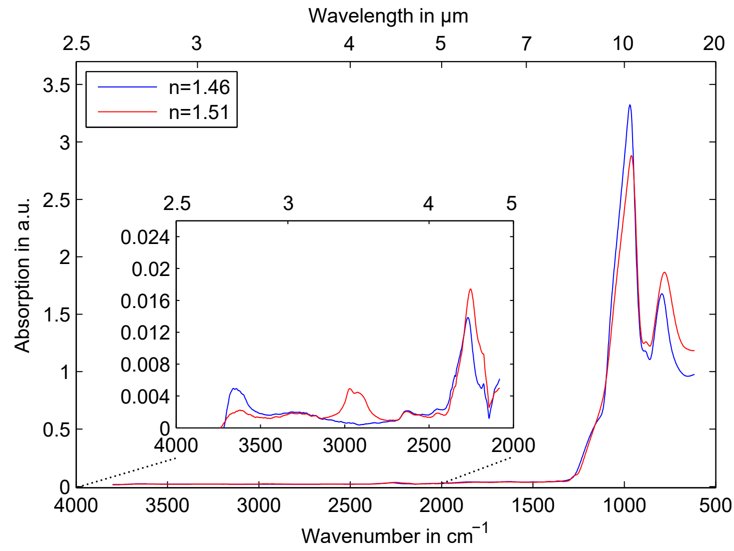

Fig. 5. ATR FTIR Spectrum of the waveguide core and cladding material.

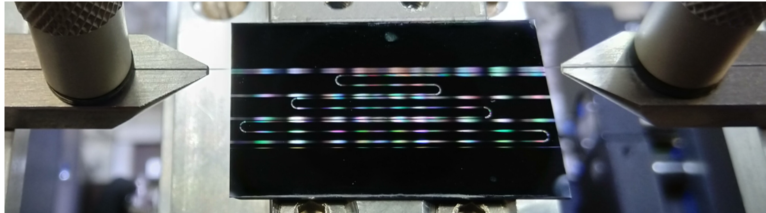

Fig. 6. Photo of the photonic chip lying on the vacuum holder with fibers positioned at the chip facets.

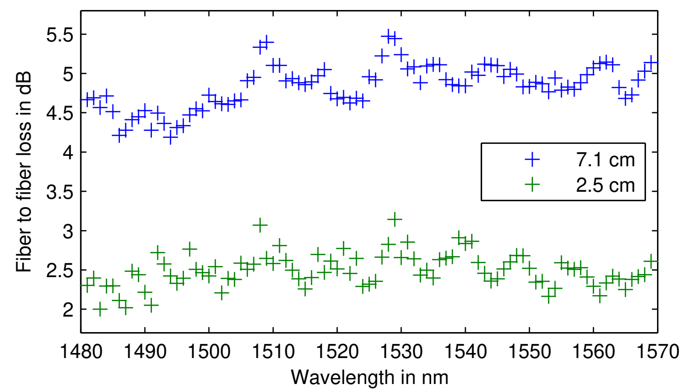

Fig. 7. Transmission spectra of waveguides with the lengths 2.5 cm and 7.1 cm.

Optical Materials EXPRESS

The coupling losses show no dependence on the wavelength and have an average value of 0.7 dB per facet. The results for the waveguide attenuation are depicted in Fig. 8. A fitting curve is added to emphasize the shape. The fluctuations over the wavelength as seen in Fig. 7 and Fig. 8 cannot be explained by material absorption or waveguide scattering. Especially the periodicity of the transmission spectrum of the waveguide with a length of 2.5 cm points to a superposition of signals with different group delays. These other propagation modes can be explained by weakly guided cladding modes excited at the fiber-to-chip interface and waveguide irregularities due to fabrication tolerances. A Fabry-Perot effect due to a gap at the fiber-chip interface can be excluded, because a gap of a few hundred µm would be necessary to produce a periodicity like in the measured spectra. However, the average error is ±0.05 dB/cm which is sufficient to confirm our claims.

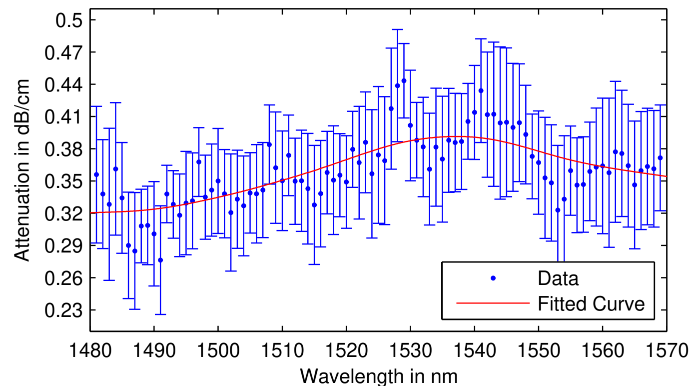

Fig. 8. Optical attenuation of SiOC waveguides with a refractive index contrast of 0.05.

An attenuation maximum is observed at 1537 nm and can be attributed to the absorption by the Si-H bond which is in agreement with the ATR FTIR data. The maximum absorption of the stretching vibrational mode of the Si-H bond is at 2165 $\text{cm}^{-1} \mathrel{\hat{=}} 4620$ nm as previously shown in Fig. 1. This causes a second overtone at $1/3 \cdot 4620$ nm = 1540 nm. The impact of the Si-H bonds on the waveguide attenuation is estimated to be below 0.1 dB/cm by comparing the maximum attenuation to the attenuation around the distant wavelength of 1480 nm where an absorption by Si-H bonds is not expected. This implies that about 0.3 db/cm of the attenuation can be attributed to scattering losses due to fabrication tolerances and sidewall roughness.

SiON waveguides fabricated with a high temperature annealing process with the same refractive index profile have attenuations between 0.05 and 0.6 dB/cm in the same wavelength range [12]. While SiOC waveguides have a lower attenuation around 1510 nm where remaining N-H bonds absorb in the SiON, SiON waveguides show better values in the C band. A waveguide attenuation of 0.29 dB/cm over the complete C band was reported for deuterated SiON waveguides with a comparable refractive index contrast [14]. This result is in agreement with the measured waveguide attenuations at wavelengths with a sufficient distance to the Si-H absorption maximum. In our case, the low losses were achieved without expensive deuterated precursor gases and without a high temperature annealing process which can lead to stress induced cracks and other issues.

Commercial silicon based low-loss waveguide technologies which rely on germanium doped silica [22] and SiN [9] can enable significantly lower losses in comparison to the values determined in this study. However, the SiOC technology provides the special feature of a wide refractive index tuneability and does not rely on high temperature processes.

Optical Materials EXPRESS

4. Conclusions

We have shown by experimental investigations that low-loss SiOC waveguides can be realized without a high temperature annealing process or deuterated precursor gases. A waveguide attenuation from around 0.3 to 0.4 dB/cm for wavelengths between 1480 and 1570 nm was measured. The quantity of Si-H bonds absorbing in the optical C band can be reduced by lowering the gas flow ratio SiH_4/CH_4. The refractive index of SiOC can be adjusted over a significantly greater range when compared to SiON. A low surface roughness over the complete refractive index range was measured by AFM. These findings make PECVD SiOC an ideal material for hybrid technologies [20] in which optical waveguides need to have a specific refractive index for example to prevent reflections at interfaces or enable low coupling losses. This study created a basis for future work which should focus on the realization of optical devices benefiting from this versatile waveguide material.

Funding

Deutsche Forschungsgemeinschaft (DFG) (501100001659).

Acknowledgments

We acknowledge financial support by Deutsche Forschungsgemeinschaft and Technische Universität Dortmund/TU Dortmund University within the funding programme Open Access Publishing.

References

1. T. Barwicz, M. A. Popovic, P. T. Rakich, M. R. Watts, H. A. Haus, E. P. Ippen, and H. I. Smith, "Microring-resonator-based add-drop filters in sin: fabrication and analysis," Opt. Express **12**(7), 1437–1442 (2004).
2. G.-L. Bona, R. Germann, and B. J. Offrein, "Sion high-refractive-index waveguide and planar lightwave circuits," IBM J. Res. Dev. **47**(2.3), 239–249 (2003).
3. B. Stern, X. Ji, A. Dutt, and M. Lipson, "Compact narrow-linewidth integrated laser based on a low-loss silicon nitride ring resonator," Opt. Lett. **42**(21), 4541–4544 (2017).
4. D. Geuzebroek, A. van Rees, E. Klein, and K. Lawniczuk, "Ultra-wide band (400-1700nm) integrated spectrometer based on arrayed waveguide gratings for spectral tissue sensing," Proc. IEEE 14th International Conference on Group IV Photonics (GFP'17), pp. 83, 84, (2017).
5. A. Leinse, L. Wevers, D. Marchenko, R. Dekker, H. R. G. R. M. Ruis, D. J. Faber, T. G. van Leeuwen, K. B. Kim, and K. Kim, "Spectral domain, common path oct in a handheld pic based system," Proc. SPIE **10483**, 104831J (2018).
6. J. Capmany, B. Ortega, D. Pastor, and S. Sales, "Discrete-time optical processing of microwave signals," J. Lightwave Technol. **23**(2), 702–723 (2005).
7. T. J. Kippenberg, R. Holzwarth, and S. A. Diddams, "Microresonator-based optical frequency combs," Science **332**(6029), 555–559 (2011).
8. M. A. Porcel, F. Schepers, J. P. Epping, T. Hellwig, M. Hoekman, R. G. Heideman, P. J. van der Slot, C. J. Lee, R. Schmidt, and R. Bratschitsch, "Two-octave spanning supercontinuum generation in stoichiometric silicon nitride waveguides pumped at telecom wavelengths," Opt. Express **25**(2), 1542–1554 (2017).
9. D. J. Blumenthal, R. Heideman, D. Geuzebroek, A. Leinse, and C. Roeloffzen, "Silicon nitride in silicon photonics," Proc. IEEE **106**(12), 2209–2231 (2018).
10. H. Ou, "Different index contrast silica-on-silicon waveguides by pecvd," Electron. Lett. **39**(2), 212–213 (2003).
11. B. E. Little, "A vlsi photonics platform," Proc. Optical Fiber Communications Conference (OFC'03), ThD1, (2003).
12. M. Fadel, M. Bülters, M. Niemand, E. Voges, and P. M. Krummrich, "Low-loss and low-birefringence high-contrast silicon-oxynitride waveguides for optical communication," J. Lightwave Technol. **27**(6), 698–705 (2009).
13. F. G. Johnson, O. S. King, J. V. Hryniewicz, L. G. Joneckis, S. T. Chu, and D. M. Gill, "Use of deuterated gases for the vapor deposition of thin films for low-loss optical devices and waveguides," (2004). US Patent 6,771,868.
14. T. Hiraki, T. Aihara, H. Nishi, and T. Tsuchizawa, "Deuterated sin/sion waveguides on si platform and their application to c-band wdm filters," IEEE Photonics J. **9**(5), 1–7 (2017).
15. F. G. Johnson, O. S. King, D. M. Gill, T. J. Davidson, and W. P. Berk, "Silicon-oxycarbide high index contrast, low-loss optical waveguides and integrated thermo-optic devices," (2006). US Patent 7,043,133.
16. S. Gallis, M. Huang, H. Efstathiadis, E. Eisenbraun, A. E. Kaloyeros, E. E. Nyein, and U. Hommerich, "Photoluminescence in erbium doped amorphous silicon oxycarbide thin films," Appl. Phys. Lett. **87**(9), 091901 (2005).
17. F. A. Memon, F. Morichetti, C. Somaschini, G. Iseni, and A. Melloni, "Experimental analysis of silicon oxycarbide thin films and waveguides," Proc. SPIE **10242**, 1024212 (2017).

Optical Materials EXPRESS

18. M. J. Loboda and J. A. Seifferly, "Method for producing hydrogenated silicon oxycarbide films having low dielectric constant," (2000). US Patent 6,159,871.
19. S. Gallis, V. Nikas, E. Eisenbraun, M. Huang, and A. E. Kaloyeros, "On the effects of thermal treatment on the composition, structure, morphology, and optical properties of hydrogenated amorphous silicon-oxycarbide," J. Mater. Res. Technol. **24**(08), 2561–2573 (2009).
20. L. Baudzus and P. M. Krummrich, "Efficient low-loss adaptive optical filters based on silicon oxycarbide - liquid crystal hybrid technology," Proc. Optical Fiber Communications Conference (OFC'19), Th2A.3, (2019).
21. T. Barwicz and H. A. Haus, "Three-dimensional analysis of scattering losses due to sidewall roughness in microphotonic waveguides," J. Lightwave Technol. **23**(9), 2719–2732 (2005).
22. A. Himeno, K. Kato, and T. Miya, "Silica-based planar lightwave circuits," IEEE J. Sel. Top. Quantum Electron. **4**(6), 913–924 (1998).